Boltzmann equation analysis of electron-molecule collision cross sections in water vapor and ammonia

M. Yousfi, and M. D. Benabdessadok

Citation: Journal of Applied Physics **80**, 6619 (1996); doi: 10.1063/1.363785
View online: https://doi.org/10.1063/1.363785
View Table of Contents: http://aip.scitation.org/toc/jap/80/12
Published by the American Institute of Physics

Boltzmann equation analysis of electron-molecule collision cross sections in water vapor and ammonia

M. Yousfi and M. D. Benabdessadok
Université Paul Sabatier, CPAT, Unité Associée au CNRS n° 277, 118 Route de Narbonne, 31062 Toulouse Cédex, France

(Received 24 May 1996; accepted for publication 9 September 1996)

Sets of electron-molecule collision cross sections for H_2O and NH_3 have been determined from a classical technique of electron swarm parameter unfolding. This deconvolution method is based on a simplex algorithm using a powerful multiterm Boltzmann equation analysis established in the framework of the classical hydrodynamic approximation. It is well adapted for the simulation of the different classes of swarm experiments (i.e., time resolved, time of flight, and steady state experiments). The sets of collision cross sections that exist in the literature are reviewed and analyzed. Fitted sets of cross sections are determined for H_2O and NH_3 which exhibit features characteristic of polar molecules such as high rotational excitation collision cross sections. The hydrodynamic swarm parameters (i.e., drift velocity, longitudinal and transverse diffusion coefficients, ionization and attachment coefficients) calculated from the fitted sets are in excellent agreement with the measured ones. These sets are finally used to calculate the transport and reaction coefficients needed for discharge modeling in two cases of typical gas mixtures for which experimental swarm data are very sparse or nonexistent (i.e., flue gas mixtures and gas mixtures for rf plasma surface treatment). © *1996 American Institute of Physics.* [S0021-8979(96)04724-X]

I. INTRODUCTION

In recent years, studies of plasma physics and gaseous electronics have been substantially stimulated by the increasing number of engineering applications such as plasma reactors for waste treatment or plasma surface treatment. Among the gases used in most of these applications, water vapor (H_2O) and/or ammonia (NH_3) are often present. When the amount of H_2O or NH_3 is not negligible, the characteristics of the plasma transport phenomena can be significantly affected by their presence. In particular, the electron swarm characteristics (velocity distribution function, ionization and attachment rates, drift velocity, diffusion coefficients, etc.) may be more or less influenced, depending on the composition of the background gas.

Reliable electron swarm data (transport coefficients and some time reaction rates) in pure gases are readily found in the literature (Dutton,[1] Gallagher *et al.*,[2] etc.). However, relevant data concerning complex mixtures or certain highly reactive gases that may be of interest for practical applications are rather sparse. To remedy this deficiency, swarm data are often derived in a gas mixture from the known data in the parent gases, by linear averages weighted on partial pressures. However, this method may lead to large errors, particularly when the atoms or molecules of the mixed gases have very different electron collision properties (Wootton and Chantry).[3]

A more appropriate method to obtain the electron swarm data in gas mixtures is to use a microscopic approach (i.e., Boltzmann's equation solution or Monte Carlo simulation) based on collision cross sections. In this case, a reliable set of electron-molecule collision cross sections for each individual component must be known. Generally, the experimental or theoretical values of cross sections available in the literature are sparse and affected by quite large uncertainties. So they are not adequate to form a complete set for microscopic calculations. Therefore, in order to obtain a complete and coherent set of cross sections in each individual gas, it is necessary to adjust these values so as to fit the experimental swarm coefficients with the calculated ones (Engelhart *et al.*,[4] Crompton *et al.*,[5] Phelps,[6] etc.).

This cross-section fitting procedure (or swarm unfolding technique) has been already applied to numerous gases (noble gases, N_2, O_2, CO_2, SF_6, etc.). In H_2O and NH_3, Hayashi[7,8] have proposed tentative sets; in the present work, these sets have been checked, but the derived swarm parameters are not in a satisfactory agreement with experimental values (see Sec. IV). Therefore, the cross-section data have been reviewed and better fit sets have been worked out, in order to obtain a good agreement between more recent swarm measurements and Boltzmann's equation calculations derived from these fitted sets.

In Sec. II, the Boltzmann method for the calculation of the hydrodynamic swarm parameters, as used in the present article, is discussed. It is based on the recent developments of the kinetic theory for the hydrodynamic regime. The technique of swarm unfolding cross sections using a simplex algorithm is also described.

In Sec. III, the actual fitted collision cross sections are reported and compared to available data. Computed results relative to electron swarm data in H_2O, NH_3, and some of their mixtures, are presented and discussed in Sec. IV.

II. METHOD OF SWARM PARAMETER CALCULATIONS

A. Introduction

The usual electron swarm parameters (drift velocity W, longitudinal, and transverse diffusion coefficients D_L and D_T, ionization and attachment frequencies $\langle \nu_{\text{ion}} \rangle$ and $\langle \nu_{\text{att}} \rangle$,

ionization and attachment coefficients α and η) are average macroscopic quantities which can be mainly measured in two distinct classes of swarm experiments.

In the first class, the steady state Townsend (SST) experiment, a stationary flux of electrons is established in the space between two electrodes. In this case, the electron number density depends only on the position within the gap. The so-called SST swarm coefficients α and η and, in some cases D_T, can be derived from this experiment.

In the second class, the time of flight (TOF) experiment, a pulsed swarm of electrons, emitted from the cathode, develops across the gap. Here, the electron number density depends upon both time and position. The so-called TOF swarm coefficients $\langle \nu_{\text{ion}} \rangle$, $\langle \nu_{\text{att}} \rangle$, W, D_T, and D_L can thus be derived from time-resolved and space-integrated measurements. The coefficients α and η can also be determined from the values of the TOF parameters.

A detailed description of both types of swarm experiments as well as a discussion on the physical meaning of the swarm parameters have been reported by many authors (Huxley and Crompton,[9] Gilardini,[10] Hunter and Christophorou,[11] Tagashira,[12] Yousfi *et al.*,[13,14] etc.).

In both classes, measurements of the electron swarm characteristics are performed far enough from the drift tube walls (compared to the electron mean free path) and on a long time scale (compared to the electron mean free time of flight). These experimental conditions correspond to the basic assumptions of the hydrodynamic approximation discussed in the following paragraph, which allows the calculation of the swarm coefficients under realistic conditions for both classes of swarm experiments.

B. Theoretical formulation

The electron swarm parameters can be calculated as average quantities in relation with the electron statistical distribution function $f(\mathbf{r},\mathbf{v},t)$ which generally depends on position $\mathbf{r}$, velocity $\mathbf{v}$, and time t. This distribution function satisfies to the Boltzmann conservation equation

$$\{\partial/\partial t + \mathbf{v}\nabla_{\mathbf{r}} + \gamma\nabla_{\mathbf{v}}\} f(\mathbf{r},\mathbf{v},t) = NJf(\mathbf{r},\mathbf{v},t), \tag{1}$$

where γ is the electron acceleration due to the external electric field and $NJf(\mathbf{r},\mathbf{v},t)$ is the scattering term. The latter accounts for the balance between the electrons scattered into and out of the elementary volume $d\mathbf{r}d\mathbf{v}$ of the phase space $(\mathbf{r},\mathbf{v})$ due to electron-molecule collisions.

The complete solution of Eq. (1) in the general case is rather difficult. However, in order to calculate the swarm parameters consistent with the experimental conditions, some simplifications can be introduced concerning the temporal and spatial dependence of the streaming term [left side term of Eq. (1)]. The theoretical approach to these simplifications (hydrodynamic approximation) has been previously described (Yousfi *et al.*,[13] Yousfi).[14] It is based on an expansion of the distribution function $f(\mathbf{r},\mathbf{v},t)$ in series of density gradients, as proposed by Kumar *et al.*:[15]

$$f(\mathbf{r},\mathbf{v},t) = \sum_{i=0}^{i=\infty} \mathbf{F}^{(i)}(\mathbf{v}) \otimes (-\nabla_{\mathbf{r}})^i n(\mathbf{r},t), \tag{2}$$

where the ith order normalized distribution function $\mathbf{F}^{(i)}(\mathbf{v})$ is a tensorial quantity that no longer depends on time t and space $\mathbf{r}$. The electron number density is defined as

$$n(\mathbf{r},t) = \int f(\mathbf{r},\mathbf{v},t)d\mathbf{v}$$

and the symbol $\otimes$ represents the i-fold scalar product.

In order to calculate the TOF swarm coefficients, it is necessary to take into account expansion (2) up to the second order. When introduced in Eq. (1), it is possible to show (in the case of an infinite space corresponding the space integrated TOF conditions) that Boltzmann's equation splits into a hierarchy of three kinetic equations. In spherical coordinate system (v,θ,ϕ) where the direction $\theta=0$ coincides with γ, with the assumption $\mu=\cos(\gamma,\mathbf{v})=\cos\theta$, the ith order kinetic equation takes the form

$$\left(\gamma\mu\frac{\partial}{\partial v} + \gamma(1-\mu^2)\frac{\partial}{v\,\partial\mu} + \Omega^{(0)} - NJ\right)F^{(i)}(v,\mu) = S^{(i)}(v,\mu). \tag{3}$$

The ith order distribution function $F^{(i)}(v,\mu)$ is assumed to be independent on the azimuthal angle ϕ. $\Omega^{(O)}$ represents the effective ionization frequency, including ionization and attachment. $S^{(i)}(v,\mu)$ is a known source term which depends on the ith order of the kinetic equation.

The TOF swarm coefficients can be derived from the distribution function $F^{(i)}(v,\mu)$ calculated up to the second order ($i=0$ for $\langle \nu_{\text{ion}} \rangle$ and $\langle \nu_{\text{att}} \rangle$, $i=1$ for W and $i=2$ for D_T and D_L).

Moreover, in order to calculate the SST swarm parameters, only the zero-th order of expansion (2) has to be taken into account. Furthermore, the time dependence of the electron density $n(\mathbf{r},t)$ disappears due to the stationary conditions. With the reference to the above spherical coordinate system, the Boltzmann's Eq. (1) can be put in the form

$$\left(\gamma\mu\frac{\partial}{\partial v} + \gamma(1-\mu^2)\frac{\partial}{v\,\partial\mu} + v\,\mu(\alpha-\eta) - NJ\right)F^{(i)}(v,\mu) = 0. \tag{4}$$

In order to solve both Eqs. (3) and (4), some additional simplifications have to be introduced for the scattering term $NJF^{(i)}$. As in the swarm experiments, the gas is only weakly ionized, it is possible to assume that the electron collisions are binary, local, and instantaneous. This means that collisions between charged particles are neglected and that electrons collide only with ground state molecules as well as certain excited ones, the latter accounting for super-elastic collisions. Furthermore, scattering is assumed isotropic. However, in order to include indirectly the effect of the collision anisotropy, the elastic momentum transfer cross section has been considered instead of the elastic cross section. Under these conditions, the scattering term can be expressed in the form

$$NJF^{(i)}(v,\mu) = -\nu(v)F^{(i)}(v,\mu) + NKF_0^{(i)}(v), \tag{5}$$

where $\nu(v)$ is the total microscopic collision frequency and $F_0^{(i)}(v)$ the isotropic part of the ith order distribution func-

tion $F^{(i)}(v,\mu)$. The term $\nu(v)F^{(i)}(v,\mu)d\mathbf{r}d\mathbf{v}$ in Eq. (5) represents the number of electrons scattered out of the volume $d\mathbf{r}d\mathbf{v}$ of the phase space and it includes the complete distribution function. The term $NKF_0^{(i)}(v)d\mathbf{r}d\mathbf{v}$ represents the number of electrons scattered into $d\mathbf{r}d\mathbf{v}$ which depends only of the isotropic part $F_0^{(i)}(v)$ of the distribution function. In the present work, the scattering term involves elastic collisions (with Davydov operator for energy exchange and thermal motion of the molecules), inelastic, and super elastic collisions. The explicit expressions of the corresponding terms have been reported in a previous article (Yousfi and Chatwiti).[16]

C. Numerical solution

Due to the effective ionization term [$\Omega^{(0)}$ or $v\mu(\alpha-\eta)$] and the collision terms, integro-differential in Eqs. (3) and (4) are nonlinear. They bear the same form and therefore have to be solved by using the same half-range iterative direct method. The numerical scheme is based on a finite difference scheme coupled to a powerful acceleration procedure (see e.g., Yousfi)[14] which gives accurate solutions with a very reduced number of iterations.

D. Monte Carlo method

The structure of the cross section in H_2O and NH_3 presents a critical region between about 0.01 up to 10 eV (see Sec. III) which leads to a strong anisotropy in the distribution functions characterized by a rapid change for small field variations (particularly for E/N range from 10 up to 100 Td). Such an effect has been already emphasized by Ness and Robson[17] in the case of water vapor. It is explained as a quasi-runaway phenomena of electrons which, for this E/N range, can gain a lot of energy before being braked by inelastic processes (vibrational and electronic excitations). Therefore, the Boltzmann calculations are very sensitive and obviously the classical two-term method fails.

In order to confirm the validity of the present multiterm Boltzmann calculations in such discharges (in H_2O and NH_3), the swarm characteristics have also been calculated by using a Monte Carlo method. The corresponding code has been developed in the frame of a previous work (Yousfi *et al.*)[18] concerning an infinite medium following the conditions of both TOF and SST swarm parameter calculations. The Monte Carlo principle used for these calculations is based on the well-known null-collision method (Skullerud).[19] The sampling technique for diffusion coefficients has been derived from Penetrante *et al.*[20]

E. Technique of swarm unfolding cross sections

The swarm parameters depend on collision cross sections, indirectly via the distribution function and directly in certain cases. This dependence is expressed by the classical known integral relationships having the following forms in the case of, for example, mean energy $\langle\epsilon\rangle$, drift velocity W, and ionization $\langle\nu_{\text{ion}}\rangle$ or attachment $\langle\nu_{\text{att}}\rangle$ frequency:

$$\langle\epsilon\rangle=\int F^{(0)}(\mathbf{v})\,\frac{1}{2}\,mv^2 d\mathbf{v}, \tag{6a}$$

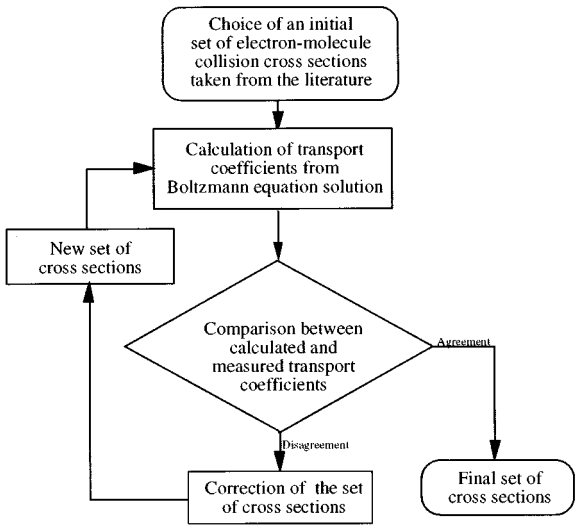

FIG. 1. Simplified flowchart of the fitting method of collision cross sections from Boltzmann equation solution.

$$W=\int F^{(0)}(\mathbf{v})v\mu d\mathbf{v}+N\int F^{(1)}(\mathbf{v})[\sigma_{\text{ion}}(v)-\sigma_{\text{att}}(v)]d\mathbf{v}, \tag{6b}$$

$$\langle\nu_{\text{ion}}\rangle=\int F^{(0)}(\mathbf{v})v\,\sigma_{\text{ion}}(v)d\mathbf{v}, \tag{6c}$$

$$\langle\nu_{\text{att}}\rangle=\int F^{(0)}(\mathbf{v})v\,\sigma_{\text{att}}(v)d\mathbf{v}, \tag{6d}$$

where $\sigma_{\text{ion}}(v)$ and $\sigma_{\text{att}}(v)$ represent the ionization and attachment collision cross sections.

The dependence between swarm parameters and collision cross sections is therefore highly nonlinear. From these relations, it is then possible to obtain the cross section by unfolding the integral relations (6). This is undertaken by a fitting method provided the swarm parameters [i.e., left-hand side of relations (6)] are known. However, due to the complex dependence of collision cross sections as a function of electron kinetic energy, the solutions of Eq. (6) are not unique. Hence, to eliminate the nonrealistic solutions, it is necessary to deduce the seeked cross section from several swarm parameter relations measured over a large E/N range. The fitting cross section technique consists of choosing and completing, for the studied gas, available data on cross sections. For the gas of our interest (H_2O and NH_3), as we will see in Sec. III, the lack of cross sections generally concerns momentum transfer cross section and cross section of certain excited states. The fitting procedure can be schematically summarized in the flowchart of Fig. 1. We start from an initial set of cross sections taken partly from the literature and completed with cross sections whose shapes obey to the theory of cross sections (see Sec. III). Then, the calculated swarm parameters from this initial set are compared to the measured ones. The initial set is modified using a simplex algorithm (see e.g., Nelder and Mead)[21] until the required coherence between measured and calculated swarm parameters is obtained. As already emphasized, the solution set is

certainly not unique but as the comparisons concern several kinds of swarm parameters having different dependencies on cross sections (ionization α/N or attachment η/N coefficients, drift velocity W, transverse D_T/μ or longitudinal D_L/μ characteristic energy) over a wide range of E/N, most of the incoherent solutions are rejected.

The simplex algorithm already used elsewhere in the case of cross section fitting (see e.g., Morgan)[22] can be summarized as follows. We optimize a function of n variables, which is in our case the minimization of the relative error χ^2 in swarm data given below:

$$\chi^2_{\mathrm{TOF}}=\sum_{i=1}^{I}\left[\left(\frac{W_{\mathrm{cal}}(E_i/N)-W_{\mathrm{mes}}(E_i/N)}{W_{\mathrm{mes}}(E_i/N)}\right)^2+\left(\frac{D_T/\mu_{\mathrm{cal}}(E_i/N)-D_T/\mu_{\mathrm{mes}}(E_i/N)}{D_T/\mu_{\mathrm{mes}}(E_i/N)}\right)^2\cdots\right],$$

$$\chi^2_{\mathrm{SST}}=\sum_{i=1}^{I}\left[\left(\frac{\alpha/N_{\mathrm{cal}}(E_i/N)-\alpha/N_{\mathrm{mes}}(E_i/N)}{\alpha/N_{\mathrm{mes}}(E_i/N)}\right)^2+\left(\frac{\eta/N_{\mathrm{cal}}(E_i/N)-\eta/N_{\mathrm{mes}}(E_i/N)}{\eta/N_{\mathrm{mes}}(E_i/N)}\right)^2\right].$$

The subscripts cal and mes correspond to respectively the calculated and measured swarm data in the case of either TOF experiment (χ^2_{TOF}) or SST experiment (χ^2_{SST}). The different E_i/N values correspond to the discretized E/N range for subscript i lying between $i=1$ up to I. The n variable corresponds to the n different cross section shapes of the considered process (for example the momentum transfer or ionization cross section, etc.) taken for the different discrete values of energy ϵ_m with $m=1$ up to n.

In fact, the simplex is started with an initial choice of cross section $\sigma_j(\epsilon_m)$ with $j=0$ up to n and $m=1$ up to n. $\sigma_0(\epsilon_m)$ is taken from the literature and the other cross sections $\sigma_j(\epsilon_m)$ with $j\neq 0$ are derived from $\sigma_0(\epsilon_m)$ using a linear transformation (Morgan).[22] Then, when the function χ^2 is minimized, the cross section coming from the final simplex fulfill the required coherence between measured and calculated swarm data.

III. COLLISION CROSS SECTIONS

It is to be noted that, due to the specific molecular structure of water vapor and ammonia, their electron-molecule collision cross sections present some similarities which induce similar behaviors in regard to electron transport (see Sec. IV). Indeed, water vapor (asymmetric top) and ammonia (symmetric top) are both polar molecules. They are therefore particularly characterized by a high rotational excitation and high momentum transfer cross sections at low energy (lower than 0.1 eV).

Furthermore, the electron-molecule collision cross sections given in this section have been mainly derived from published data in the literature. However, in some cases the cross sections available have been adjusted using a simplex method in order to obtain the best coherence between the calculated and measured swarm parameters. The sets of cross sections presented in this article as the result of the fitting procedure, must therefore be considered as a coherent and inseparable sets. They can be used as a powerful tool to calculate macroscopic transport characteristics of electrons in H_2O or NH_3 and their mixtures.

A. Water vapor collision cross sections

1. Rotational and vibrational excitation cross sections

Only very few and sparse experimental data are available in the literature on rotational excitation of water molecule. The theoretical calculations based on Born approximations (Itikawa,[23] Jain and Thompson[24]) have been used as a basis for the present fittings [Fig. 2(a)]. The cross-section thresholds and shapes have been taken from the results of these authors. As their calculations are performed in different energy ranges, the cross sections have been joined (when it is possible) together to cover a relatively extended energy range. However, an important scaling factor has been introduced to reduce the magnitude of these cross sections, in order to fit the calculated transport parameters at low E/N. In fact, only the transitions between some low-lying rotational states have been considered. All the higher level transitions have been grouped into a single fitted cross section with a threshold of about 0.073 eV corresponding to 0–7 transitions [Fig. 2(a)].

As far as the vibrational excitation is concerned, the experimental results of Seng and Linder[25] have been considered, together with those derived from a semi-analytic calculation scheme (Olivero *et al.*)[26] and by Born approximation calculations (Itikawa).[27] There are also in the literature the experimental data of Shyn *et al.*[28] and the calculations of Nishimura and Itikawa[29] which are in agreement with those of Send and Linder.[25]

The cross sections for the excitation of the fundamentals of the stretching modes [(000)→(100),(001) with thresholds of 0.435 and 0.466 eV] and the bending mode (000→(010) with threshold of 0.198 eV) have been taken into account. They have been grouped into two excitation functions, according to the experimental values of Seng and Linder[25] [Fig. 2(a)]. The other vibrational transitions have been neglected, because their cross sections are lower by more than one order of magnitude (Olivero *et al.*).[26]

2. Excitation cross sections of optical levels

A large amount of data has been collected in the literature on the structure of the water molecule and on the energy configuration of its different electronic states. However, data derived from optical observations (e.g., Herzberg)[30] and from inelastic electron scattering (e.g., Claydon *et al.*,[31] Trajmar *et al.*,[32] Lassettre and White)[33] are not always in agreement. In particular, the characteristics of the triplet state $^3B_1$ are not definitively assessed.

In fact, the excited states taken into account in the present work can be summarized following a schematic energy level diagram already reported by Olivero *et al.*[26] (Fig. 1 of Olivero *et al.*) and updated for the present work according to more recent results. This energy diagram can be described as follows.

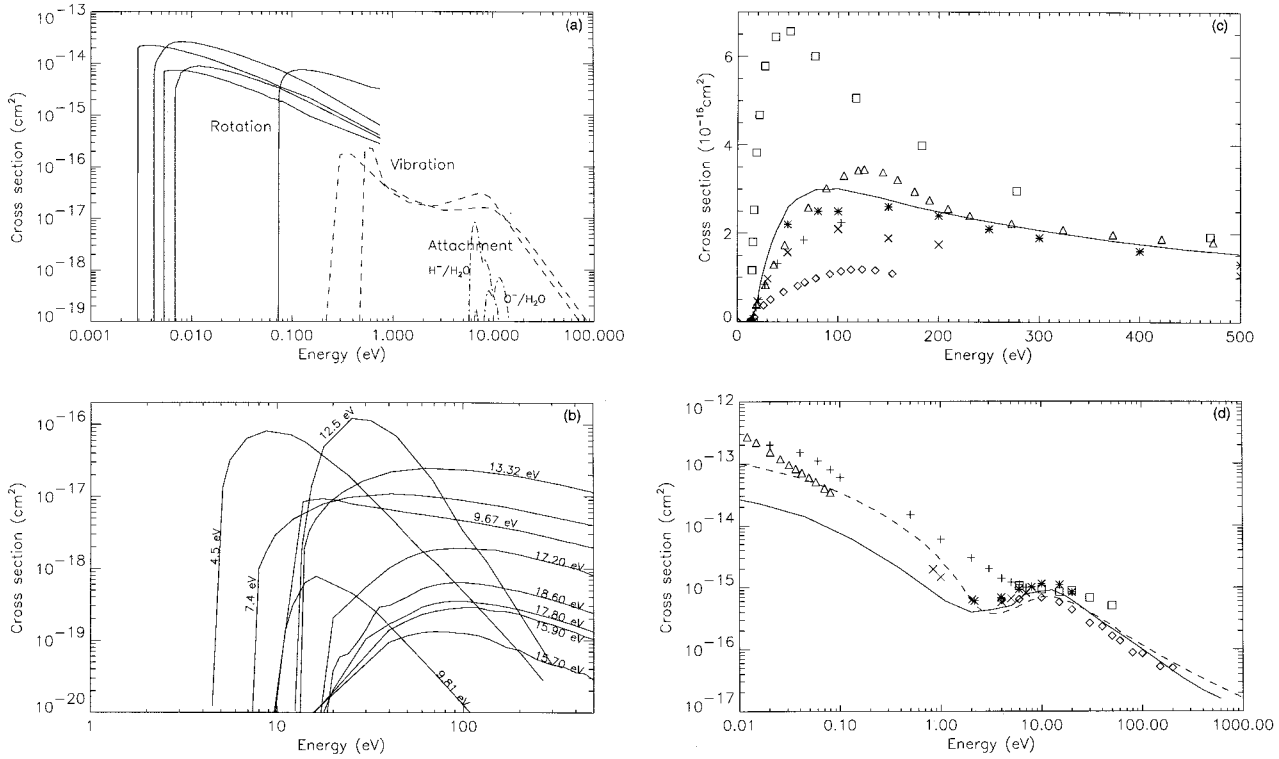

FIG. 2. (a) Overview on some electron-molecule collision cross sections for H_2O: Five rotational excitations (—), two vibrational excitations (- - -), and dissociative attachment: H^-/H_2O, O^-/H_2O. (b) Excitation cross sections with the corresponding energy thresholds for some electronic states of electron-H_2O collision. (c) Ionization collision cross sections of H_2O by electron impact: Bolorizadeh and Rudd (Ref. 37) (*), Gomet (Ref. 36) (△), Ness and Robson (Ref. 17) (+), Mark and Egger (Ref. 68) (◇), Schutten *et al.* (Ref. 35) (×), Vriens (Ref. 80) (□), and present work (—). (d) Momentum transfer cross sections for electron-H_2O collision: Present work (—), Hayashi (- - -), Sokolov and Sokolova (Ref. 42) (+), Danjo and Nishimura (Ref. 41) (◇), Seng and Linder (Ref. 23) (×), Pack *et al.* (Ref. 40) (△), Johnston and Newell (Ref. 51) (□), Shyn and Cho (Ref. 52) (*).

Below the ionization threshold (12.62 eV), the four Rydberg series A $(npa1\ ^1B_1)$, B $(npb1\ ^1A_1)$, C $(nsa1\ ^1B_1)$, and D (nd) are taken into account.

For lower energies, the two singlet states $\tilde{A}\ ^1B_1$ (7.4 eV) and $\tilde{B}\ ^1B_1$ (9.67 eV) are included. As both states are not bounded, they lead to dissociation respectively to $H(2s)+OH(X\ ^2\Pi)$ and $O(1d)+H_2(X\ ^1\Sigma_g^+)$ and their excitational envelope, corresponding to the vibrational stretching and bending modes of the singlet $\tilde{X}\ ^1A_1$ ground state, is relatively extended.

The two triplet states $\tilde{A}\ ^3B_1$ (7.02 eV) and $\tilde{A}\ ^3B_2$ (9.81 eV) are then added. Both states are related dissociatively to $H(2s)+OH(X^2\Pi)$ and $O(2p^4 3p)+H_2(X\ ^1\Sigma_g^+)$. However, while the $^3B_2$ are surely dissociative, the excitation envelope of the $^3B_1$ state seems to extend down to 4.5 eV, indicating the existence of a few bounded vibrational levels (Claydon *et al.*,[31] Klump and Lassettre).[34]

Above the ionization threshold, a few broad bonds have been observed in optical studies (Watanabe and Jursa).[35] They are situated around 13.32 eV.

A number of dissociative excitation processes are possible in water vapor. Some of the most important of these transitions have been taken into account in the present work

$$e+H_2O(X\ ^1A_1)\rightarrow H(1s)+OH(A\ ^2\Sigma^+):OH(A\ ^2\Sigma^+\rightarrow X\ ^2\Pi) \quad (9.67\ \text{eV})$$

$$e+H_2O(X\ ^1A_1)\rightarrow H(3s)+OH(X\ ^2\Pi):H_I\ \text{Balmer}\ \alpha \quad (17.8\ \text{eV})$$

$$e+H_2O(X\ ^1A_1)\rightarrow H(4s)+OH(X\ ^2\Pi):H_I\ \text{Balmer}\ \beta \quad (18.6\ \text{eV})$$

$$e+H_2O(X\ ^1A_1)\rightarrow H(2p)+OH(X\ ^2\Pi):H_I\ \text{Lyman}\ \alpha \quad (17.2\ \text{eV})$$

$$e+H_2O(X\ ^1A_1)\rightarrow O(3p\ ^3P)+H_2(X\ ^1\Sigma_g^+):O_I(3p\ ^3P\rightarrow 3s\ ^3S^0) \quad (15.9\ \text{eV})$$

$$e+H_2O(X\ ^1A_1)\rightarrow O(3p\ ^5P)+H_2(X\ ^1\Sigma_g^+):O_I(3p\ ^5P\rightarrow 3s\ ^5S^0) \quad (15.7\ \text{eV}).$$

The cross sections for all the above listed processes are reported as a function of the electron energy in Fig. 2(b) with the corresponding thresholds and the original references (Beenaker *et al.*[36] and Böse).[37] In Fig. 2(b), further excitation cross sections of dissociative state (thresholds at 7.4 and 13.32 eV), and of triplet states (thresholds at 4.5 and 9.81 eV) taken both from Olivero *et al.*[26] work are also shown.

Further data on excitation cross sections can be found in articles of Mohlmann *et al.*,[38] Lee *et al.*[39] and Gil *et al.*[40]

In Fig. 2(b), an additional cross-section σ_{fic} is reported with the threshold at 12.5 eV, which includes all the Rydberg transitions (of series A, B, C, and D) and all the other excitation processes which are not considered individually in this section. This cross section has been fitted in order to obtain a good agreement between computed and measured transport coefficients.

3. Ionization and attachment cross sections

The data on the total ionization cross section available in the literature are relatively abundant and consistent (Schutten *et al.*,[41] Gomet,[42] Bolorizadeh and Rudd,[43] Dolan[44] etc.). However, in the present work, slightly higher values have been used [Fig. 2(c)], in order to obtain consistent values more particularly for the ionization coefficient in the lower field region.

The main processes for dissociative attachment in water vapor have been reviewed by Compton and Christophorou.[45] The two major ones

$$e+H_2O\rightarrow H^-+OH \quad (5.7\ \text{eV})$$
$$e+H_2O\rightarrow O^-+H_2 \quad (4.9\ \text{eV})$$

have been considered in the present work. The cross section for H^- formation has been derived from the results of these authors, while that for O^- has been obtained from the data of Melton and Neece.[46] The magnitude of H^-/H_2O cross section has been slightly adjusted to fit the experimental total attachment coefficient and also drift velocity, particularly for the E/N range lying between 10 and 100 Td.

4. Elastic momentum transfer and total cross section

Figure 2(d) shows some of the more recent values of the momentum transfer cross section σ_m and of the total cross-section σ available in the literature in comparison with the values fitted in the present work.

In the low energy range (below 1 eV), no direct experimental data of σ_m are available. Pack *et al.*[47] have derived the momentum transfer cross section from drift velocity measurements. However, their values are higher than the present fitting because these authors in their σ_m derivation did not take into account the rotational excitation, which has a very low threshold in H_2O. For this reason, their values may rather be considered as a total cross section.

In the intermediate energy range (between 1 and 10 eV), the actual σ_m fittings are consistent with the experimental values reported in the literature and present a sort of Ramsauer minimum around 2.5 eV and a resonance maximum at about 10 eV.

For higher energies (up to 200 eV), the present σ_m values decrease with a slope coherent with data reported by Danjo and Nishimura.[48]

The fitted values of the total cross-section σ are quite comparable to the experimental results reported in the literature (Sokolov and Sokolova,[49] Brüche,[50] Johnston and Newell,[51] and Shyn and Cho).[52] There are also numerous calculations of σ_m [not reported in Fig. 1(d)] whose shapes are quite coherent with experimental data (see e.g., Machado *et al.*,[53] Okamoto *et al.*,[54] Rescigno and Lengsfiel,[55] Sato *et al.*,[56] Gianturco and Thompson,[57] etc.).

B. Ammonia collision cross sections

1. Rotational and vibrational excitation cross sections

Here also, only very few data can be found in the literature in the case of electron impact rotational excitation cross sections for NH_3 molecule. The present data are derived in the framework of Born approximation adapted by Itikawa[58] to the case of interactions between electron and symmetric-top molecules. It can be observed in Fig. 3(a) for NH_3 (which is a polar molecule like H_2O), that rotational excitation cross sections are far from being negligible compared to the other excitation cross sections and can reach several tens of 10^{-16} cm^2. In fact, the rotational transitions having weak cross sections are not taken into account due to their negligible effect on electron transport.

Data on vibrational excitation cross sections are very sparse. Those corresponding to energy thresholds 0.12, 0.201, 0.414, and 0.427 eV (see Hertzberg)[30] are calculated using Born approximation as considered by Takayanagi.[59] The magnitude of such cross sections [see Fig. 3(a)] are then fitted and their shapes are adapted to those given by Hayashi[8] to obtain the best agreement between experimental and calculated transport coefficients at low E/N regions corresponding to the low electron kinetic energy range.

2. Electronic excitation cross sections

As in the case of numerous molecular gases, excitation cross sections of optical levels are not really abundant in the literature even though several articles are devoted to the studies of electron-impact spectra (Skerbele and Lassettre)[60] or dissociation (Muller and Schulz,[61] Fukui *et al.*,[62] Bubert and Froben)[63] or light emission particularly in the VUV range.[64] In fact, the main drawbacks to include such electronic processes is first to choose the most important ones for electron transport and then to find reliable cross sections in the literature. In this article, some electron-NH_3 reactions mainly for dissociative excitation processes have been selected from the literature with their corresponding thresholds:

$$e+NH_3\rightarrow NH+H_2 \quad (3.9\ \text{eV})$$
$$e+NH_3\rightarrow NH_2+H \quad (5.6\ \text{eV})$$
$$e+NH_3\rightarrow NH+{}_2H \quad (8.6\ \text{eV}).$$

Excitation cross sections σ_{ex} for certain electronic transitions, needed for reaction rate calculations, can be taken

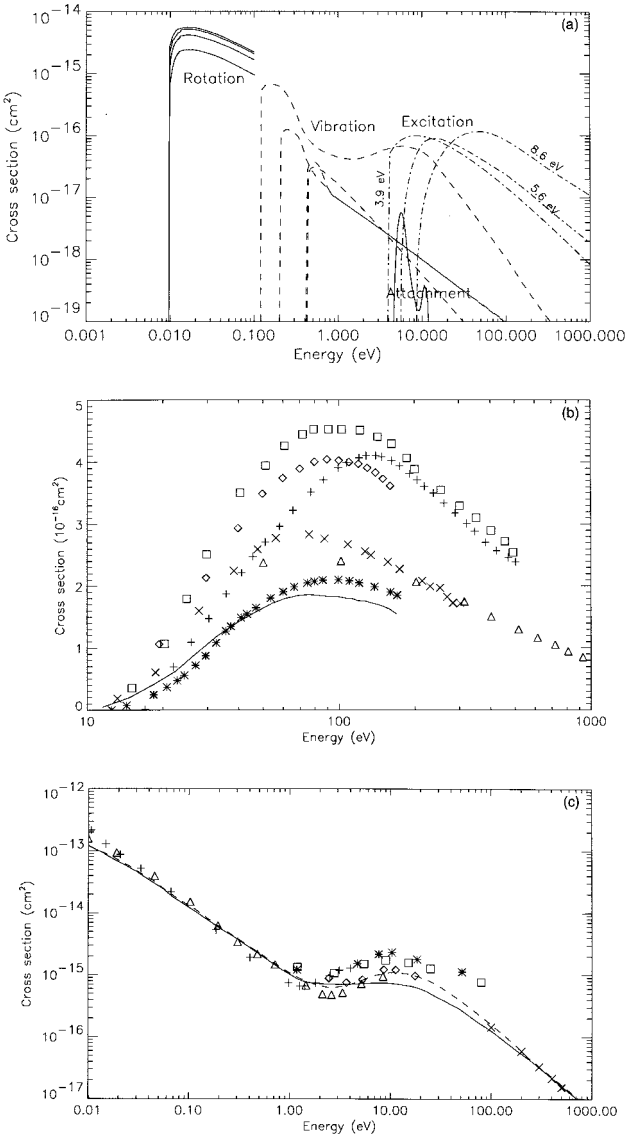

FIG. 3. (a) Overview on some electron-molecule collision cross sections for NH_3: Four rotational excitations (—), four vibrational excitations (- - -), three electronic excitations (-·-·-), and dissociative attachment. (b) Ionization collision cross sections of NH_3 by electron impact: Mark *et al.* (Ref. 68) used for present work (—), Gomet (Ref. 36) (+), Djuric-Preger *et al.* (Ref. 66) (◇), Jain and Khare (Ref. 69) (*), Crowe and McConkey (Ref. 70) (×), Bederski (Ref. 71) (△), Orient and Srivastava (Ref. 67) (□). (c) Momentum transfer cross sections for electron-NH_3 collision: Present work (—), Hayashi (Ref. 8) (- - -), Jain and Thompson (Ref. 22) (+), Compilation of Itikawa (Ref. 25) (△), Szmythkowski *et al.* (Ref. 81) (□), Sueoka *et al.* (Ref. 82) (*), Jain *et al.* (Ref. 73) (×), Pritchard *et al.* (Ref. 74) (◇).

from measurements of Muller and Schulz.[61] However, their magnitude are too low to affect electron transport. The different excitation cross sections used in present work are shown in Fig. 3(a).

3. Ionization and attachment cross sections

There are numerous measurements and semi-empirical calculations of total and partial ionization cross sections of NH_3 by electron impact (see e.g., the article of Khare and Meath[65] with its references). In fact, ionization cross section data can be divided in two groups. Those measured by Gomet,[36] or Djuric-Preger *et al.*,[66] or Orient and Srivastava[67] which give total ionization cross sections quite coherent but which are higher than data given by another group of authors such as Mark *et al.*,[68] or Jain and Khare,[69] or Crowe and Mc Konkey,[70] or Bederski *et al.*[71] In this article, we have used the total ionization cross section given by Mark *et al.*[68] because it gives the best fit with measured ionization coefficients. Figure 3(b) gives an overview on some different total ionization cross sections found in the literature.

Furthermore, the reader interested by partial ionization cross sections for formation of several ions by electron-NH_3 impacts (NH_3^+, NH_2^+, NH^+, H^+, N_2^+, N^+, H_2^+), necessary for partial ionization rate calculations, can find in the literature measurements of Gomet[36] or those of Mark *et al.*[68]

The cross sections for dissociative attachment (H^- and NH_2^- ion formation) are taken from measurements of Compton *et al.* given in the compilation of Laborie *et al.*[72]

4. Elastic momentum transfer and total cross section

As in the H_2O case, there are in the literature several data given by different authors for momentum transfer cross section. We can note several calculations: those of Jain and Thompson[22] from 0.01 up to 10 eV updated and completed by Jain *et al.*[73] from 0.1 up to 1000 eV, those calculated by Pritchard *et al.*[74] from 2.5 to 20 eV, those compiled by Itikawa[25] and also those given by Hayashi.[8] In fact, these different data are not really consistent. In the present work, the elastic momentum transfer cross section obtained by fitting is quite close to the data given in the literature at low energy (lower than about 0.5 eV) and for high energy (higher than 100 eV) but is quite different from data of the literature particularly in the Ramsauer minimum energy range from around 1 eV up to 10 eV. Figure 3(c) shows an overview on some different data present in the literature of elastic and also total collision cross section compared with present elastic momentum transfer cross section.

IV. RESULTS AND DISCUSSION

A. Electron transport coefficients in H_2O and NH_3

Figures 4(a)–4(e) show, respectively, drift velocity W, longitudinal eD_L/μ and transverse eD_T/μ characteristic energies, α/N ionization and η/N attachment coefficients for electrons in H_2O. In these figures, the transport coefficients calculated from actual fitted set of H_2O cross sections (see Sec. III) are compared with experimental swarm data and also with transport coefficients calculated using Hayashi's set of cross sections. It can first be noted that transport coefficients calculated from our selected set of cross sections are, as a consequence of the fitting procedure, in quite nice agreement with experimental swarm data (lower than 2% for the drift velocity and lower than 10% for characteristic energy i.e., of the same order of magnitude as the experimental uncertainties). However, in the case of the attachment coefficient, the deviations between calculations and measurements observed for $E/N>100$ Td lead to a less satisfying agreement. It is probably due to some collisional processes such as electronic detachment not included in our calculations. We also observe the nonrealistic behavior of the attachment co-

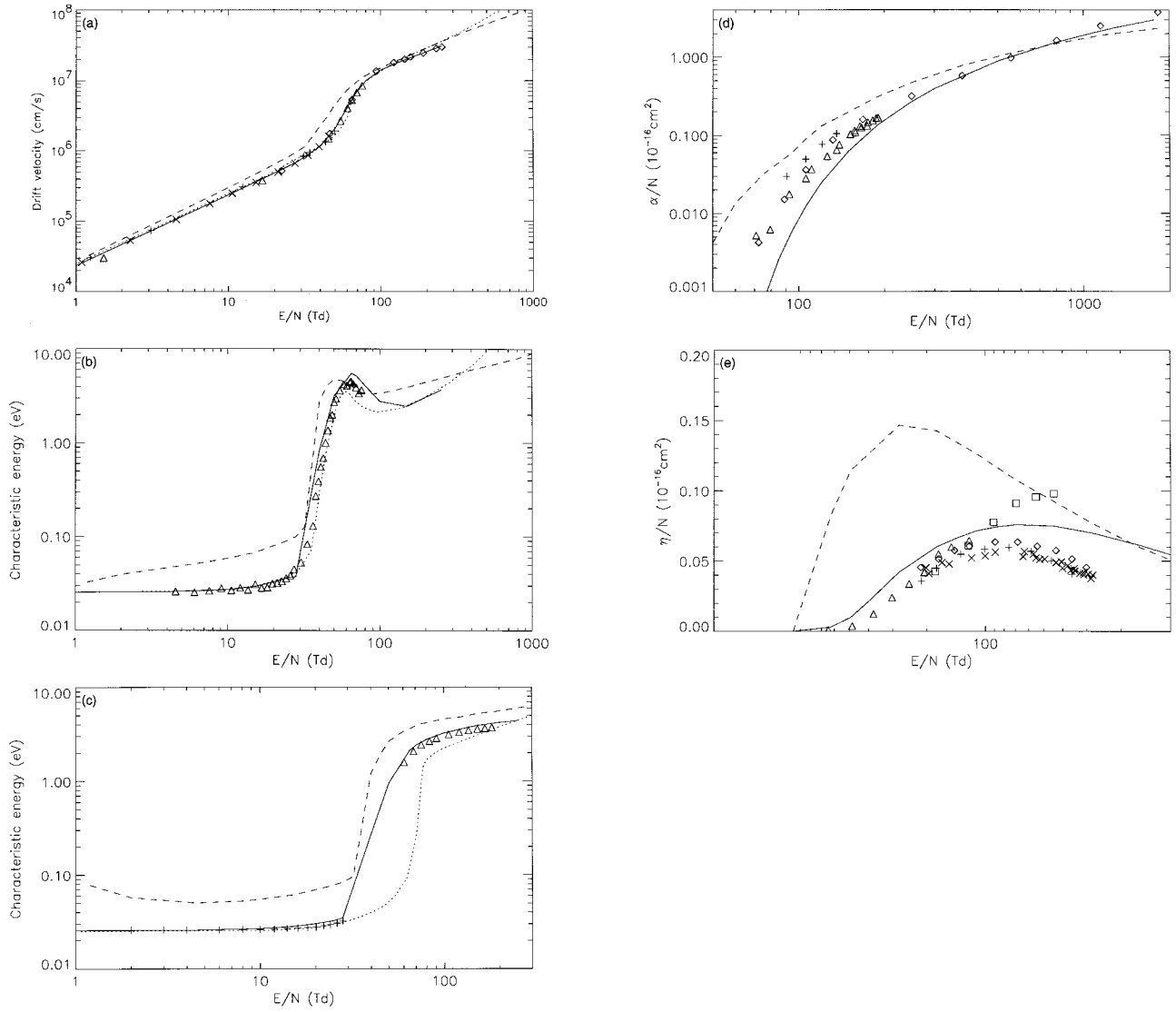

FIG. 4. (a) Drift velocity for electrons in H_2O: Symbols: Measurements from Wilson *et al.* (Ref. 83) (△), Pack *et al.* (Ref. 40) (+), Lowke and Rees (Ref. 84) (×), Ryzko (Ref. 85) (◇); Lines: Boltzmann equation calculations for T_{gas}=293 K from set of present work cross sections (—), from Hayashi's (see Ref. 7) set (- - -), and from Ness and Robson's (see Ref. 17) set (·····). (b) Longitudinal characteristic energy of electrons in H_2O; Symbols: Measurements from Wilson *et al.* (see Ref. 83) (△); Lines: Boltzmann equation calculations for T_{gas}=293 K from set of present work cross sections (—), from Hayashi's (see Ref. 7) set (- - -) and from Ness and Robson's (see Ref. 7) set (·····). (c) Transversal characteristic energy of electrons in H_2O: Symbols: Measurements from Crompton *et al.* (see Ref. 5) (△) and Elford (see Ref. 86) (+); Lines: Boltzmann equation calculations for T_{gas}=293 K from set of present work cross sections (—), from Hayashi's (see Ref. 7) set (- - -) and from Ness and Robson's (see Ref. 17) set (·····). (d) Total ionization coefficients for electrons in H_2O; Symbols: measurements from Prasad and Craggs (see Ref. 75) (+), Ryzko (see Ref. 85) (△), Risbud and Naidu (see Ref. 87) (◇); Lines: Boltzmann equation calculations for T_{gas}=293 K from set of present work cross sections (—), from Hayashi's (see Ref. 7) set (- - -), and from Ness and Robson's (see Ref. 17) set (·····). (e) Dissociative attachment coefficients for electrons in H_2O; Symbols: measurements from Parr and Moruzzi (see Ref. 76) (△), Prasad and Craggs (see Ref. 75) (□), Ryzko (see Ref. 85)(×), Risbud and Naidu (see Ref. 87) (+), and Crompton *et al.* (see Ref. 5) (◇); Lines: Boltzmann equation calculations for T_{gas}=293 K from set of present work cross sections (—), from Hayashi's (see Ref. 7) set (- - -), and from Ness and Robson's (see Ref. 17) set (·····).

efficient of Prasad and Craggs[75] which continually increases with E/N; this can be due to the presence of electronegative molecular impurities. In Fig. 4, we can also observe that the swarm data calculated using Hayashi's set of cross sections are not close to the measured swarm data whatever the E/N range. Furthermore, when the set of collision cross sections taken from Ness and Robson[17] is considered in our Boltzmann equation calculations, we obtain a better agreement with experimental swarm data (particularly at low E/N range) than the cross section set of Hayashi. However, even though more satisfying results can be obtained by considering the anisotropy scattering of elastic collision (see Ness and Robson), there are always some deviations—difficult to ignore—between experimental and calculated swarm data (see transverse characteristic energy) thus justifying the new fitting of H_2O collision cross sections undertaken in this article, to update the existing cross sections. Furthermore, as the present H_2O set of collision cross sections is intended to be used, in a next step, for transport and reaction coefficient calculations in gas mixtures, the assumption of the isotropic scattering instead of the anisotropic one is certainly more simple to use for gas mixtures. However, the anisotropy of collisions is not completely ignored in our calculations because, as known, the use of momentum transfer cross section

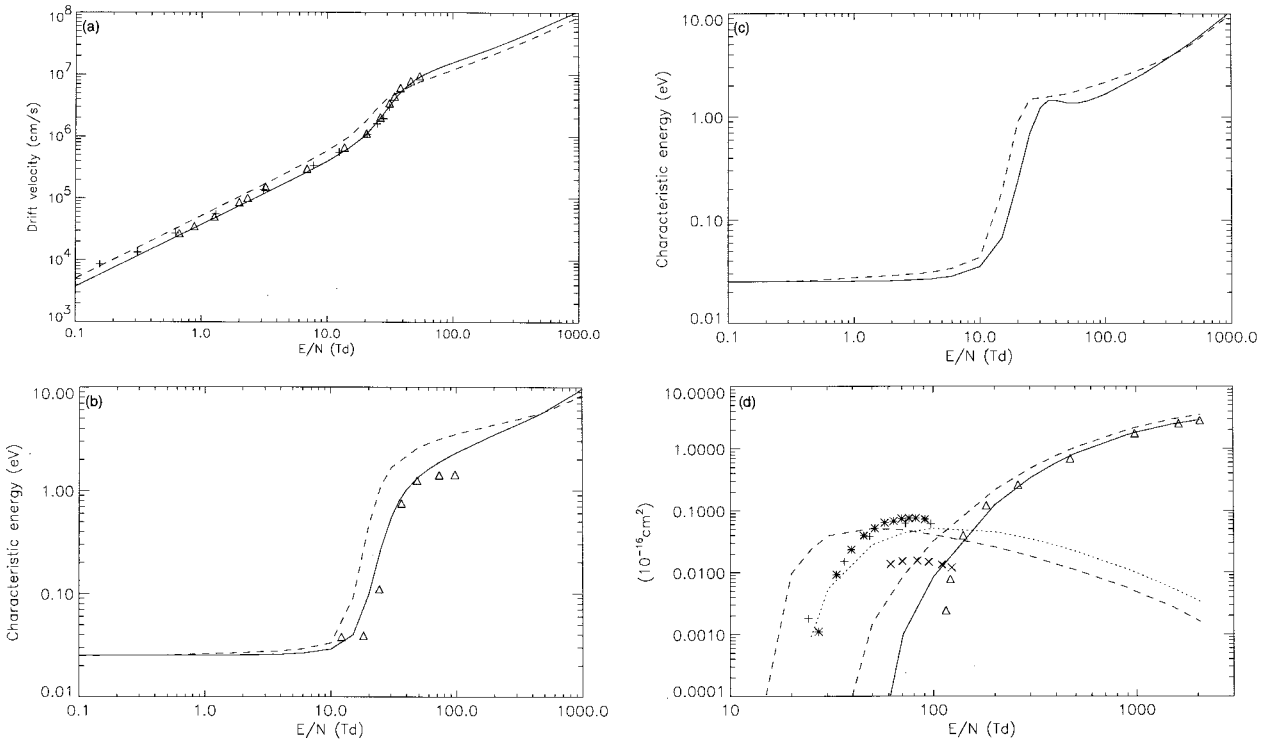

FIG. 5. (a) Drift velocity for electrons in Symbols: measurements from Nielsen and Bradbury (see Ref. 88) (△) and Pack *et al.* (see Ref. 40) (+); Lines: Boltzmann equation calculations for T_{gas}=293 K from set of present work cross sections (—) and from Hayashi's (see Ref. 8) set (- - -). (b) Transversal characteristic energy of electrons in NH_3; Symbols: measurements from Bailey and Ducanson (see Ref. 89) (△); Lines: Boltzmann equation calculations for T_{gas}=293 K from set of present work cross sections (—) and from Hayashi's (see Ref. 8) set (- - -). (c) Longitudinal characteristic energy of electrons in NH_3; Boltzmann equation calculations for T_{gas}=293 K from set of present work cross sections (—) and from Hayashi's (see Ref. 8) set (- - -). (d) Dissociative attachment (·····) and total ionization (—) coefficients for electrons in NH_3; Symbols: Measurements from Bailey and Ducanson (see Ref. 89) (+), Risbud and Naidu (see Ref. 87)(×, △), and Parr and Moruzzi (see Ref. 76) (*); Lines: Boltzmann equation calculations for T_{gas}=293 K from cross sections of present work, (- - -) from Hayashi's (see Ref. 8) set of cross sections.

instead of the elastic collision cross section can partly take into account the anisotropy of collisions (see e.g., Yousfi.[14])

Then, Figs. 5(a)–5(d) show, respectively, drift velocity W, longitudinal eD_L/μ and transverse eD_T/μ characteristics energies, α/N ionization and η/N attachment coefficients for electrons in NH_3. The calculated swarm data are compared to experimental ones except in the case of eD_L/μ where, to the authors' knowledge, there are no experimental data available in the literature. Here, we also note, as a consequence of the present cross section fitting, the quite nice agreement between our results and the experimental swarm data. However, the measured attachment coefficients, coming from two different references (Refs. 76 and 87), present a similar shape but not the same magnitude [see Fig. 5(c)]. We observe that our calculations are in better coherence with Parr and Morruzi's[76] measurements.

In both cases (H_2O and NH_3), the behavior of electron transport data present some similitudes. Indeed, in the case of characteristic energies (eD_L/μ or eD_T/μ), we observe three E/N ranges already emphasized by Ness and Robson[17] in the case of H_2O. In the first range (below ~25–30 Td for H_2O and 15–20 Td for NH_3), electron energy is quasithermal. This is due to the high magnitude of inelastic and superelastic processes of rotational transitions. Then, in the second E/N range (up to about 80 Td for H_2O and 50 Td for NH_3), the electron transport is strongly affected by the rapid decrease of elastic and rotational excitation cross sections so that the electron energy increases very rapidly from the quasithermal energy up to an energy higher by 2 orders of magnitude. This is called a quasi-runaway effect by Ness and Robson.[17] Then, in the third E/N range, this rapid rise is slowed down as vibrational and electronic excitations begin to intervene. These three E/N ranges are also observable in drift velocity behavior [see Figs. 4(a) and 5(a)], which represents the anisotropy of the electron swarm as a function of E/N. In the drift velocity W case, the three E/N ranges is characterized by three different slopes of W. We observe, in particular, in the second E/N range, the faster increase of electron swarm anisotropy due to the rapid failure of elastic and rotational excitation collisions previously emphasized. Further calculations based on Monte Carlo simulation show that the relaxation time τ_r (the time necessary for electrons starting from their initial conditions to reach an equilibrium between energy and momentum transfer lost by collisions and gained by the field) for the second E/N range is (unlike classical gases not presenting this quasi-runaway effect) higher than τ_r corresponding to the first E/N range. This can always be explained by the rapid decrease of the total collision frequency which is inversely proportional to the relaxation time.

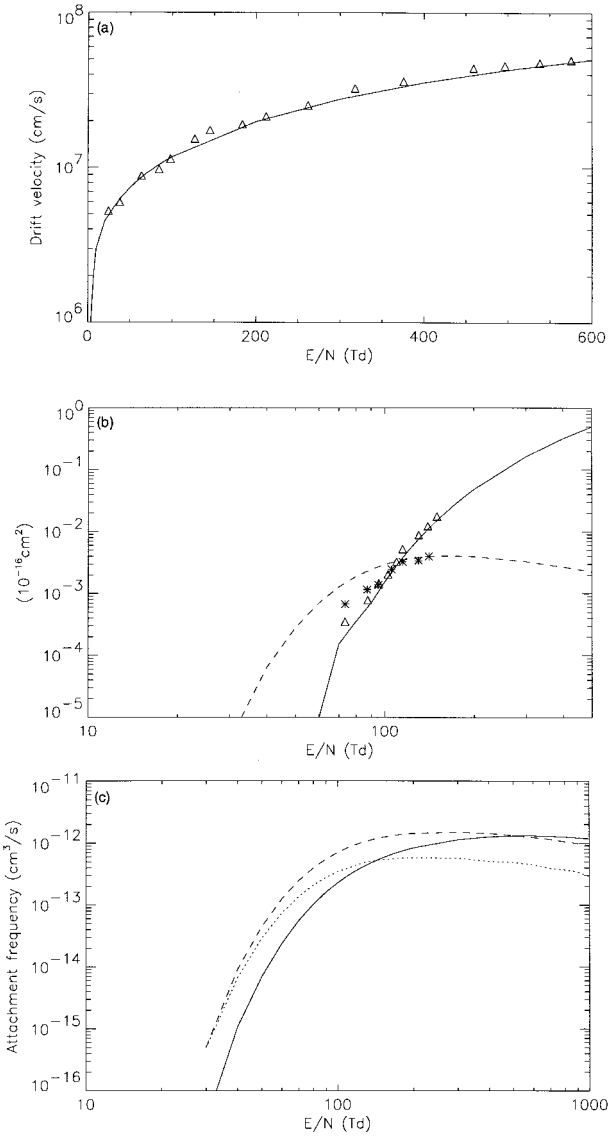

FIG. 6. (a) Electron drift velocity in flue gas *B* (74% N_2, 15% CO_2, 6% H_2O, 5% O_2) for T_{gas}=300 °K; Symbols: measurements from Verhaart (see Ref. 77) (△); Lines: Boltzmann equation calculations from set of present work cross sections (—). (b) Attachment (- - -, *) and ionization (—,△) coefficients in flue gas B (74% N_2, 15% CO_2, 6% H_2O, 5% O_2) for T_{gas}=300 °K; Symbols: measurements from Verhaart (see Ref. 77); Lines: Boltzmann equation calculations from cross sections of present work. (c) Partial attachment frequency of electrons in flue gas B (74% N_2, 15% CO_2, 6% H_2O, 5% O_2) for T_{gas}=300 °K: O^-/H_2O(—), O^-/O_2(- - -), and O^-/CO_2(·····).

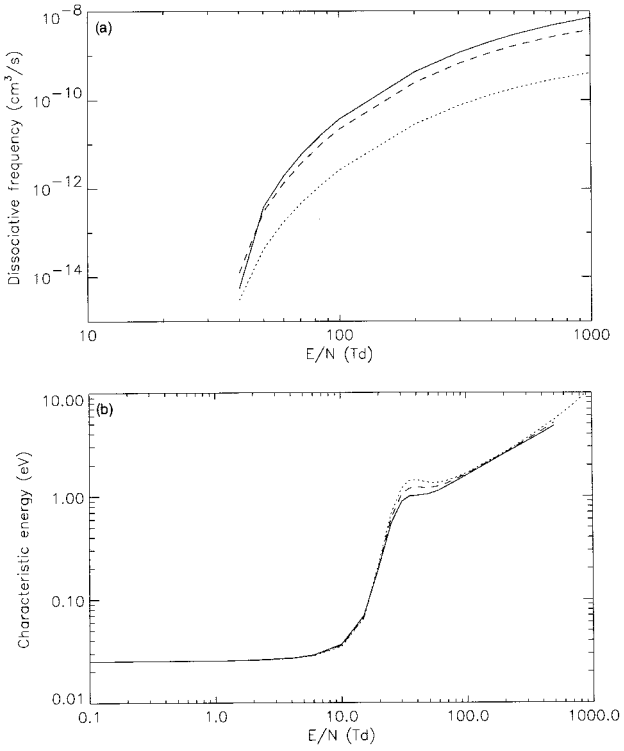

FIG. 7. (a) Dissociation frequency of SiH_4 in SiH_4/NH_3 mixtures by electron impacts for T_{gas}=300 °K: 10% of SiH_4(—), 5% of SiH_4(- - -), and 0.5% of SiH_4(·····). (b) Longitudinal characteristic energy of electrons in SiH_4/NH_3 mixtures for T_{gas}=300 °K: 10% of SiH_4(—), 5% of SiH_4(- - -), and 0.5% of SiH_4(·····).

B. Transport coefficients in typical gas mixtures involving H_2O and NH_3

In this section, electron swarm data are calculated from Boltzmann equation solution using the fitted H_2O and NH_3 sets of collision cross sections in two typical cases of gas mixtures: those involved in nonthermal plasma applications for pollution control of flue gases ($N_2-O_2-H_2O-CO_2$ mixtures) and those used for plasma surface treatment using rf discharges or other sources of excitations of the gas mixtures (as e.g., SiH_4-NH_3).

Figures 6(a) and 6(b) show drift velocity and ionization and attachment coefficients in a typical flue gas resulting from coal burning. The composition of this flue gas, called flue gas B by Verhaart[77] and already used by Gallimberti[78] in his model, is 74% N_2, 15% CO_2, 6% H_2O, and 5% O_2. The electron-molecule collision cross sections used for N_2, CO_2, and O_2 come from Yousfi *et al.*[79] compilation. Our Boltzmann calculations are quite well compared to time resolved measurement of Verhaart.[77] To the authors' knowledge, Verhaart's measurements are the only experimental data available in the case of flue gases. So, in order to obtain, for example the partial attachment coefficients (see Fig. 6(c) showing attachment frequency for O^- ion formation by electron impact on H_2O, O_2, and CO_2 in the mixture) for the two mixtures analyzed by Verhaart or the transport and reaction coefficients for other flue gases with different gas compositions, the Boltzmann equation calculations constitute the unique alternative.

Figures 7 show an example of transport and reaction coefficients (dissociation frequency of SiH_4 by electron impact and drift velocity) useful for rf discharge modeling in the case of SiH_4-NH_3 mixtures for different proportions of SiH_4 in NH_3 (0.5%, 5%, and 10%). The set of electron-SiH_4 collision cross sections used in the present calculations comes from Ohmori *et al.*[90] work and then fitted (mainly in the case of momentum transfer and electronic excitation cross sections) in order to be coherent with swarm parameter measurements given in the literature (see e.g., Ref. 90 with the associated references). The dissociation frequency as a function of E/N for both reactions [$e+SiH_4 \rightarrow e+SiH_3+H$ and $e+SiH_4 \rightarrow e+SiH_2+{}_2H$], [see Fig. 7(a)] show the well

known saturation effect when the proportion of SiH_4 in the mixture increases. This is probably why this proportion does not exceed, in the case of practical mixtures, 4% or 5% because the frequency of creation of SiH_3 radicals (which is one of the most important radicals in chemical kinetics in the plasma reactor) is efficient enough around 4% or 5% of SiH_4 in the mixture and a higher proportion does not increases significantly this efficiency. Unlike the dissociation frequency shown in Fig. 7(a), the transport coefficients are not too affected by the addition of a small quantity of SiH_4 in the mixture [see Fig. 7(b) showing characteristic longitudinal energy]. For this kind of complex gas mixture, Boltzmann equation analysis is also the unique alternative to obtain for example the partial ionization or attachment rates.

V. SUMMARY

In this article, the hierarchy of Boltzmann equations corresponding for each class of classical swarm experiments (steady state, time resolved, or time of flight) are established in the hydrodynamic approximation framework. This enables the calculations of scalar (e.g., ionization or attachment frequency), vectorial (drift velocity), and tensorial (diffusion coefficients) hydrodynamic electron swarm parameters from the knowledge of cross sections of electron-neutral collisions. The cross sections of electron-H_2O and electron-NH_3 collisions available in the literature are reviewed and the corresponding swarm parameters are analyzed using an iterative multiterm numerical solution of the Boltzmann equation. In a second step, these two sets of collision cross sections are compiled and fitted using a swarm data unfolding technique based on comparison of electron swarm parameter measurements from the two classes of swarm experiments and calculations based on Boltzmann equation solutions. A simplex optimization algorithm is used to fit the collision cross sections. Finally, the selected sets of H_2O and NH_3 cross sections are used in the case of two typical gas mixtures involved in nonthermal plasmas applications ((i) flue gas treatment using e-beam irradiation or corona discharge and (ii) plasma surface treatment with rf discharge), to calculate the transport and reaction coefficients needed for discharge modeling (i.e., modeling of charged particles dynamics and chemical kinetics of neutral and charged particles).

[1] J. Dutton J. Phys. Chem. Ref. Data **4**, 577 (1975).
[2] J. W. Gallagher, E. C. Beaty, J. Dutton, and L. C. Pitchford, J. Phys. Chem. Ref. Data **12**, 109 (1983).
[3] R. E. Wooton and P. J. Chantry, *Gaseous Dielectrics II*, edited by L. G. Christophorou (Pergamon, New York, 1980), pp. 32–42.
[4] A. G. Engelhart, A. V. Phelps, and C. G. Risk, Phys. Rev. **135**, A1566 (1964).
[5] R. W. Crompton, M. T. Elford, and R. L. Jory, Aust. J. Phys. **20**, 369 (1967).
[6] A. V. Phelps, Rev. Mod. Phys. **40**, 399 (1968).
[7] M. Hayashi, *Swarm Studies and Inelastic Electron-Molecule Collisions*, edited by Pitchford *et al.* (Springer, New York, 1985), pp. 167–187.
[8] M. Hayashi, *Nonequilibrium Processes in Partially Ionized Gases*, edited by M. Capitelli (Plenum, New York, 1989), pp. 333–340.
[9] L. G. H. Huxley and R. W. Crompton, *Diffusion and Drift of Electrons in Gases* (Wiley Interscience, New York, 1974).
[10] A. Gilardini, *Low Energy Electron in Gases* (Wiley, New York, 1972).
[11] S. R. Hunter and L. G. Christophorou, *Electron-Molecule Interactions and Their Applications*, edited by L. G. Christophorou (Academic, New York, 1985), Vol. 2, pp. 89–129.
[12] H. Tagashira, Proceedings of the Fifteenth International Conference on Phenomena on Ionized Gases, Minsk (Invited Paper) 1981 (unpublished), p. 377.
[13] M. Yousfi, P. Segur, and T. Vassiliadis, J. Phys. D **18**, 359 (1985).
[14] M. Yousfi, these de Doctorat d'Etat, n°1244, Universite Paul Sabatier Toulouse, 1986.
[15] K. Kumar, H. R. Skullerud, and R. E. Robson, Aust. J. Phys. **33**, 343 (1980).
[16] M. Yousfi and A. Chatwiti, J. Phys. D **20**, 1457 (1987).
[17] K. F. Ness and R. E. Robson, Phys. Rev. A **38**, 1446 (1988).
[18] M. Yousfi, A. Hennad, and A. Alkaa, Phys. Rev. E **49**, 3264 (1994).
[19] H. R. Skullerud, Brit. J. Phys. D: Appl. Phys. **1**, 1567 (1968).
[20] B. M. Penetrante, J. N. Bardsley, and L. C. Pitchford, J. Phys. D **18**, 1087 (1985).
[21] J. A. Nelder and R. Mead, Comut. J. **7**, 308 (1965).
[22] W. L. Morgan, Phys. Rev. A **44**, 1677 (1991).
[23] Y. Itikawa, J. Phys. Soc. Jpn. **31**, 217 (1972).
[24] A. Jain and D. G. Thompson, J. Phys. B: At. Mol. Opt. Phys. **16**, 2593 (1983).
[25] G. Seng and F. Linder, J. Phys. B: At. Mol. **9**, 2539 (1976).
[26] J. J. Olivero, R. W. Stagat, and A. E. S. Green, J. Geophys. Res. **77**, 4797 (1972).
[27] Y. Itikawa, At. Data Nucl. Data Tables **14**, 1 (1974).
[28] T. W. Shyn, S. Y. Cho, and T. E. Cravens, Phys. Rev. A **36**, 5138 (1987).
[29] T. Nishimura and Y. Itikawa, J. Phys. B: At. Mol. Phys. **28**, 1995 (1995).
[30] G. Herzberg, *Electronic Spectra of Polyatomic Molecules* (Van Nostrand, Princeton, New York, 1966).
[31] C. R. Claydon, G. A. Seagl, and H. S. Taylor, J. Chem. Phys. **54**, 3799 (1971).
[32] S. Trajmar, W. Williams, and A. Kuppermann, J. Chem. Phys. **54**, 2274 (1971).
[33] E. N. Lassettre and E. R. White, J. Chem. Phys. **60**, 2460 (1974).
[34] K. N. Klump and E. N. Lassettre, Can. J. Phys. **53**, 1825 (1975).
[35] K. Watanabe and A. S. Jursa, J. Chem. Phys. **41**, 1659 (1964).
[36] C. Beenaker, F. J. De Heer, H. B. Krop, and G. R. Mohlmann, Chem. Phys. **6**, 445 (1974).
[37] N. Böse, Phys. Lett. **65A**, 402 (1978).
[38] G. R. Mohlmann, K. H. Shima, and F. J. DeHeer, Chem. Phys. **28**, 331 (1978); G. R. Mohlmann and F. J. DeHeer, *ibid.* **40**, 157 (1979).
[39] M. T. Lee, S. E. Michelin, L. E. Machado, and L. M. Brescansin, J. Phys. B: At. Mol. Phys. **28**, 1995 (1995).
[40] T. J. Gil, T. N. Rescigno, C. W. McCurdy, and B. H. Lengsfield Phys. Rev. A **49**, 2642 (1994).
[41] J. Schutten, F. J. DeHeer, H. R. Moustafa, A. J. H. Boerbom, and J. Kistmaker, J. Chem. Phys. **44**, 3924 (1966).
[42] J. C. Gomet, C. R. Acad. Sci. B **281**, 627 (1975).
[43] M. A. Bolorizadeh and M. E. Rudd, Phys. Rev. A **33**, 882 (1986).
[44] T. J. Dolan, J. Phys. D: Appl. Phys. **24**, 3633 (1991).
[45] R. N. Compton and L. G. Christophorou, Phys. Rev. **154**, 110 (1967).
[46] C. E. Melton and G. A. Neece, J. Chem. Phys. **55**, 4665 (1971).
[47] J. L. Pack, R. E. Voshall, and A. V. Phelps, Phys. Rev. **127**, 2084 (1962).
[48] A. Danjo and H. Nishimura, J. Phys. Soc. Jpn. **54**, 1224 (1985).
[49] V. F. Sokolov and Y. A. Sokolova, Sov. Tech. Lett. **7**, 268 (1982).
[50] E. Brüche, Ann. Phys. **1**, 93 (1929).
[51] W. M. Johnstone and W. R. Newell, J. Phys. B: At. Mol. Phys. **24**, 3633 (1991).
[52] T. W. Shyn and S. Y. Cho, Phys. Rev. A **36**, 5138 (1987).
[53] L. E. Machado, L. Mu-Tao, L. M. Brescansin, M. A. P. Lima, and V. MacKoy, J. Phys. B: At. Mol. Opt. Phys. **28**, 467 (1995).
[54] Y. Okamoto, K. Onda, and Y. Itikawa, J. Phys. B: At. Mol. Phys. **26**, 745 (1993).
[55] T. N. Rescigno and B. H. Lengsfield, Z. Phys. D: At. Mol. Clusters **24**, 117 (1992).
[56] H. Sato, M. Kimura, and K. Fujima, Chem. Phys. Lett. **145**, 21 (1988).
[57] F. A. Gianturco and D. G. Thompson, J. Phys. B: At. Mol. Phys. **13**, 613 (1980).
[58] Y. Itikawa, J. Phys. Soc. Jpn. **30**, 835 (1971).
[59] K. Takayanagi, J. Phys. Soc. Jpn. **21**, 835 (1966).
[60] A. Skerbele and E. N. Lassettre, J. Chem. Phys. **42**, 395 (1965).
[61] U. Muller and G. Schulz, Chem. Phys. Lett. **138**, 385 (1987); U. Muller and G. Schulz, Chem. Phys. Lett. **170**, 401 (1990); U. Muller and G. Schulz, J. Chem. Phys. **96**, 5924 (1992).

[62] K. Fukui, I. Fujita, and K. Kuwata, J. Chem. Phys. **81**, 1252 (1977).
[63] H. Bubert and F. W. Froben, J. Chem. Phys. **75**, 769 (1971).
[64] J. Masanet, A. Gilles, and C. Vermeil, J. Photochem. **3**, 417 (1974/75); H. Morgan and J. E. Mentall, J. Chem. Phys. **60**, 4734 (1974); N. Böse and W. Sroka, Z. Naturforsch. A **26**, 1491 (1971).
[65] S. P. Khare, and W. J. Meath, J. Phys. B **20**, 2101 (1987).
[66] N. Djuric-Preger, D. Belic, and M. Kurepa, Proceedings of the Eighth Symposium on Physics of Ionized Gases, Dubrovnik, 1976, p. 54.
[67] O. J. Orient and S. K. Srivastava, *14th International Conference on the Physics of Electronic and Atomic Collisions*, Palo Alto, edited by D. C. Lorents, W. E. Meyerhof, and J. R. Peterson (North-Holland, Amsterdam, 1985), p. 274.
[68] T. D. Mark and F. Egger, Int. J. Mass Spec. Ion Phys. **20**, 89 (1976); T. D. Mark, F. Egger, and M. Cheret, J. Chem. Phys. **67**, 3795 (1977).
[69] D. Jain and S. P. Khare, J. Phys. B: At. Mol. Phys. **9**, 1429 (1976).
[70] A. Crowe and J. W. McConkey, Int. Mass Spectrom. Ion Phys. **24**, 181 (1977).
[71] K. Bederski, L. Wojcik, and B. Adamczyk, Int. Mass Spectrom. Ion Phys. **35**, 171 (1980).
[72] P. Laborie, J. M. Rocard, and J. A. Rees, in *Metallic Vapours and Molecular Gases* (Dunod, Paris, 1971); R. N. Compton, J. A. Stockdal, and P. W. Reinhard, Phys. Rev. **180**, 111 (1969).
[73] A. K. Jain, A. N. Tripathi, and A. Jain, Phys. Rev. A **39**, 1537 (1989).
[74] H. P. Pritchard, M. A. P. Lima, and V. McKoy, Phys. Rev. A **39**, 2392 (1989).
[75] A. N. Prasad and J. D. Craggs, Proc. Phys. Soc. London **76**, 223 (1960); **77**, 385 (1961).
[76] J. E. Parr and J. L. Moruzzi, J. Phys. D **5**, 514 (1972).
[77] H. F. A. Verhaart, Kema Scientific & Technical Reports **7**, 377 (1989).
[78] I. Gallimberti, Pure Appl. Chem. **60**(28), 663 (1988).
[79] M. Yousfi, N. Azzi, I. Gallimberti, and I. Stangherlin, ''Electron-molecule collision cross sections and electron swarm parameters in some atmospheric gases (N_2,O_2,CO_2, and H_2O),'' Data base collection $n°1$, Toulouse-Padova, 1987 (unpublished).
[80] L. Vriens, Proc. Phys. Soc. **89**, 13 (1966).
[81] C. Szmytkowski, K. Maciag, G. Karwasz, and D. J. Filipovic, J. Phys. B: At. Mol. Opt. **22**, 525 (1989).
[82] O. Sueoka, S. Mori, and Y. Katayama, J. Phys. B: At. Mol. Phys. **20**, 3237 (1987).
[83] J. F. Wilson, F. J. Davis, D. R. Nelson, R. N. Compton, and O. H. Crawford, J. Chem. Phys. **62**, 4204 (1975).
[84] J. J. Lowke and J. A. Rees, Aust. J. Phys. **16**, 447 (1963).
[85] H. Ryzko, Proc. Phys. Soc. London **85**, 1283 (1965); H. Ryzko, Ark. Fys. **32**, 1 (1966).
[86] M. T. Elford, *International Conference on Phenomena in Ionized Gases*, edited by W. T. Williams (University College of Swansea Press, Swansea, 1987), Vol. 1, p. 130.
[87] A. V. Risbud and M. S. Naidu, J. Phys. (France) Colloq. **40**, 77 (1979).
[88] R. A. Nielsen and N. E. Bradbury, Phys. Rev. **51**, 69 (1937).
[89] V. A. Baily and W. E. Duncanson, Philos. Mag. **10**, 145 (1930).
[90] Y. Ohmori, M. Shimozuma, and H. Tagashira, J. Phys. D: Appl. Phys. **19**, 1029 (1986).